STEM CELLS AND DEVELOPMENT
Volume 22, Number 10, 2013

DOI: 10.1089/scd.2012.0556

Coordinated Development of Voltage-Gated Na^+ and K^+ Currents Regulates Functional Maturation of Forebrain Neurons Derived from Human Induced Pluripotent Stem Cells

Mingke Song, Osama Mohamad, Dongdong Chen, and Shan Ping Yu

Like embryonic stem (ES) cells, human induced pluripotent stem (hiPS) cells can differentiate into neuronal cells. However, it is unclear how their exquisite neuronal function is electrophysiologically coordinated during differentiation and whether they are functionally identical to human ES cell-derived neurons. In this study, we differentiated hiPS and ES cells into pyramidal-like neurons and conducted electrophysiological characterization over the 4-week terminal differentiation period. The human neuron-like cells express forebrain pyramidal cell markers NeuN, neurofilament, the microtubule-associated protein 2 (MAP2), the paired box protein Pax-6 (PAX6), Tuj1, and the forkhead box protein G1 (FoxG1). The size of developing neurons increased continuously during the 4-week culture, and cell-resting membrane potentials (RMPs) underwent a negative shift from -40 to -70 mV. Expression of the muscarinic receptor-modulated K^+ currents (I_M) participated in the development of cell RMPs and controlled excitability. Immature neurons at week 1 could only fire abortive action potentials (APs) and the frequency of AP firing progressively increased with neuronal maturation. Interestingly, the developmental change of voltage-gated Na^+ current (I_{Na}) did not correlate with the change in the AP firing frequency. On the other hand, the transient outward K^+ current (I_A), but not the delayed rectifier current (I_K) contributed to the high frequency firing of APs. Synaptic activities were observed throughout the 4-week development. These morphological and electrophysiological features were almost identical between iPS and ES cell-derived neurons. This is the first systematic investigation showing functional evidence that hiPS cell-derived neurons possess similar neuronal activities as ES cell-derived neurons. These data support that iPS cell-derived neural progenitor cells have the potential for replacing lost neurons in cell-based therapy.

Introduction

Embryonic stem (ES) cells are well known for their pluripotent differentiation capacity. They can develop into diverse specialized cells, including neuronal cells, and thus have promising applications in basic developmental biology, drug discovery, disease therapies, and regenerative medicine. The translational application of human ES cells into treating diseases, however, has encountered several ethical concerns and possible immune rejection after transplantation [1]. To circumvent concerns related to the implementations of human ES cell technology, human induced pluripotent stem (hiPS) cells were generated from human somatic cells [2]. Adult somatic cells were reprogrammed into ES cell-like state by introducing crucial pluripotency genes that allow them to differentiate into different cell types. The promise offered by the hiPS cell technology has huge clinical potential for transplantation therapy without incurring the ethical controversy associated with ES cells. Neuronal differentiation of iPS cells provides a powerful new approach to study neurodevelopment, disease models, and develop new treatments for nervous system disorders. Before practical applications become reality, however, more effort is needed to thoroughly examine these converted adult cells for safety concerns as well as to better understand their competence in cell replacement therapy. To do so, a practical and reliable approach is to compare the differentiation properties of the hiPS cells with that of ES cells. So far, there have been few comparative examinations to determine differences between human iPS cells and ES cells with regard to pluripotency, gene expression, and the functional phenotypes of neurally induced cells.

A recent report demonstrated that hiPS cells differentiated into neural cells under the same conditions used for human ES cells, but with reduced efficiency and variable potency

Department of Anesthesiology, Emory University School of Medicine, Atlanta, Georgia.

between cell lines [3]. In the forebrain, mature pyramidal neurons are highly differentiated cellular elements in the nervous system, with complicated function determined by a specific spatiotemporal assembly of Na^+, K^+, and Ca^{2+} channels [4–6]. They are excitable cells with resting membrane potential (RMP) from −60 to −70 mV, and able to fire repetitive action potentials (APs) when receiving a stimulating input strong enough to activate the fast inactivating inward Na^+ currents (I_{Na}) [7,8]. The firing pattern of APs is under strict control of K^+ channel activities [9]. Among the many voltage-gated K^+ channels, the muscarinic receptor-coupled K^+ channels or KCNQ2/3 channels are activated in the membrane potential range near the threshold of evoking APs. The M-current (I_M) acts like a brake to maintain the membrane potential below the threshold for voltage-gated Na^+ channel activation, thereby controlling neuronal excitability [10]. The transient A-type K^+ currents (I_A) counteract the activation of I_{Na}, keeping the single AP short and helping neurons fire a repetitive pattern of APs [11]. The delayed rectifier K^+ currents (I_K) are responsible for cell membrane potential discharge and repolarization upon and after AP activation [12]. Different firing activities generate diverse AP propagation patterns, thus leading to a sophisticated neuronal signal coding and transmitter release. Although neuronal differentiation of hiPS cells has been demonstrated, whether differentiated cells derived from iPS cells can behave like mature neurons with exquisite coordination between voltage-gated Na^+ and K^+ channels capable of firing repetitive APs has been obscure. Such an evaluation is particularly important to determine whether hiPS cells can functionally replace human ES cells, and whether they are suitable for developmental and translational research as well as clinical applications.

Recently, we developed a feeder-free neuronal differentiation method to induce human ES and iPS cells into neural progenitor cells, and then into maturing pyramidal-like neurons over the ensuing 4 weeks. In the present study, we characterized the morphological and functional development of the pyramidal-like neurons derived from hiPS cells along the 4-week differentiation. We deciphered the key relationship between the AP firing patterns and the developmental changes in voltage-gated Na^+ and K^+ currents in hiPS cells, and compared them to neuronal features of cells differentiated from human ES cells.

Materials and Methods

Cell culture and neuronal differentiation of hiPS and ES cells

Human H1 ES cells (WiCell) and vector-free hiPS cells (iPS-DF19-9/7T, WiCell Research Institute) were routinely cultured on hES-qualified Matrigel (BD Biosciences) in a serum-free and feeder-free mTeSR medium (Stem Cell Technologies). The cells used for differentiation were no older than passages 35–55. Cells were passaged using dispase every 5 to 7 days after manual removal of differentiated colonies. For more information on the maintenance of hiPS cells with mTeSR1, please refer to the guidelines published by Stem Cell Technologies (www.stemcell.com//en/Products/Popular-Product-Lines/mTeSR-TeSR2.aspx).

Neural induction was achieved through a modification of the protocol described in Chambers et al. and our earlier report [13,14] using dorsomorphin and SB431542. Cells were dissociated using accutase (Invitrogen) for 15 min, and then plated as single cells on Matrigel-coated plates (BD Biosciences) at a density of 18,000–20,000 cells/cm^2 in mouse embryonic fibroblast-conditioned media supplemented with the 10 ng/mL basic fibroblast growth factor (bFGF; R&D System) and 10 μM ROCK inhibitor (Y27632; Sigma-Aldrich Corp.). Three to five days later, cells were confluent and the medium was changed to the knockout serum replacement (KSR) medium containing the knockout Dulbecco's modified Eagle's medium (DMEM), 15% KSR, 1% L-glutamine, 1% nonessential amino acids, and beta-mercaptoethanol supplemented with 3 μM dorsomorphin (Tocris) and 10 μM SB431542 (a transforming growth factor-β inhibitor; Stemgent). This is considered day 0 in the differentiation protocol and cells were then allowed to grow for 5 days. The medium was then changed to a 1:4 mixture of the N2 medium (DMEM/F12, N2 supplement, L-glutamine) and KSR medium, with dorsomorphin, but without SB431542. The proportion of the N2 medium was gradually increased to 50% on day 7 and 75% on day 9. On day 11, cells were dissociated with accutase, resuspended in the N2 medium, and cultured onto Matrigel-coated culture dishes with a 1:1 mixture of the N2 and B27 medium (the Neurobasal medium, B27 supplement, and L-glutamine) with 10 ng/mL of the bFGF for terminal differentiation. Media was changed every 3 days for 4 weeks.

Neuronal differentiation of mouse iPS and ES cells

Mouse primary iPS cells (WP5) were purchased from Stemgent. Mouse ES cells were prepared from stocks of the wild-type D3 ES cell line. Cells were cultured and differentiated as previously described [15]. Briefly, undifferentiated cells were maintained in T25 flasks in ES cell growth media (ESGM) consisting of the DMEM, supplemented with 10% fetal bovine serum, 10% newborn calf serum, 8 μg/mL adenosine, 8.5 μg/mL guanosine, 7.3 μg/mL cytidine, 7.3 μg/mL uridine, 2.4 μg/mL thymidine, the leukemia inhibitory factor (LIF) at 1,000 units/mL, and 0.1 mM β-mercaptoethanol. For induction of neural differentiation, one quarter of the cells from a T25 flask were seeded into a standard 100-mm bacterial Petri dish in ESGM lacking LIF and β-mercaptoethanol (ES cell induction media, [ESIM]). After 2 days, the media and cell aggregates were removed from the dish and the aggregated cells were allowed to settle for 10 min in a 15-mL centrifuge tube. The media was then aspirated and replaced. Cells were then returned to the culture dish for an additional 2 days. The culture media was then replaced with ESIM containing 5×10^{-7} M retinoic acid (RA) (all-trans RA, Sigma-aldrich), and the cells were cultured for an additional 4 days.

Immunocytochemistry

Cells were fixed with 4% paraformaldehyde for 20 min at room temperature, postfixed with a 2:1 mixture of ethanol:acetic acid, permeabilized with 0.2% Triton-X-100, and blocked with 1% fish gelatin for 1 h. Primary antibodies (diluted to 1/500 or 1/1,000) against PAX6, Tuj1 (Covance), NeuN, neurofilament (NF) (EMD Millipore Corporation), FoxG1 (Abcam), and MAP2 (Santa Cruz Biotechnology, Inc.) were applied overnight at 4°C. The next day, cells were washed 3 times in phosphate-buffered saline (PBS) and incubated with secondary Cy3- or fluorescein isothiocyanate

(FITC)-conjugated antibodies in PBS for 1 h. Hoechst 33342 (1 μg/mL; Molecular Probes) was added to stain cell nuclei. Images were visualized by fluorescence microscopy (BX61; Olympus).

Electrophysiological recordings

Whole-cell recording was performed on human ES and iPS cell-derived neurons using an EPC9 amplifier (HEKA; Elektronik) at 21°C–23°C. The external solution contained (in mM) 135 NaCl, 5 KCl, 1 $MgCl_2$, 2 $CaCl_2$, 10 HEPES, and 10 Glucose at a pH of 7.4. Recording electrodes pulled from borosilicate glass pipettes (Sutter Instrument) had a tip resistance between 5 to 8 MΩ when filled with the internal solution (in mM): 140 KCl, 2 $MgCl_2$, 1 $CaCl_2$, 2 Na_2ATP, 10 EGTA, and 10 HEPES at a pH of 7.2. Series resistance was compensated by 60%–80%. Linear leak and residual capacitance currents were subtracted on-line using a P/6 protocol. APs were recorded under the current-clamp mode using Pulse software (HEKA, Elektronik). Miniature excitatory or inhibitory postsynaptic currents (mE/IPSCs) were recorded under the voltage-clamp mode in the presence of tetrodotoxin (TTX, 1 μM). To record voltage-gated K^+ I_A and I_K currents, TTX (1 μM) and $CdCl_2$ (100 μM) were added into the external solution to suppress voltage-gated Na^+ and Ca^{2+} currents. To record pure I_{Na}, 140 mM KCl in the internal solution was replaced with 120 mM CsCl and 20 mM tetraethylammonium-chloride (TEA-Cl), and 100 μM $CdCl_2$ was added into the external solution. When recording voltage-gated Ca^{2+} currents, the internal solution for I_{Na} recordings was used, while 1 μM TTX was added into the external solution to block Na^+ currents. Data were filtered at 3 kHz and digitized at sampling rates of 20 kHz. The AP amplitude was measured from the initial threshold to the peak of the AP upstroke. The peak amplitude of I_{Na} evoked by a 0 mV voltage command was used for data analysis. The size of the M-type K^+ current (I_M) was determined by measuring the amplitude of the deactivating current induced by a 20 mV hyperpolarization step (from −30 to −50 mV). We measured the amplitude of the delayed rectifier (I_K) current at the end of a 40 mV depolarization. The amplitude of the fast inactivating K^+ current I_A was determined by measuring the peak component elicited by stepping from −120 to 0 mV. We measured the maximum amplitude of high-voltage-activated (HVA) Ca^{2+} currents elicited by the 0 mV voltage command.

Statistical analysis

All electrophysiological data in this study are expressed as mean ± SEM. Statistical comparisons between correlated groups were assessed by the Student's *t*-test. A comparison among the 3 groups was analyzed using one-way ANOVA followed by a post hoc Tukey's test.

Results

HiPS cell-derived neurons express forebrain makers

After 4-week neuronal differentiation, neuronal antibody markers were used to stain differentiated cells derived from hiPS and ES cells. Immunocytochemical staining showed expression of the NF, neuron-specific class III beta-tubulin (Tuj 1), and the mature neuronal maker neuronal nuclear antigen (NeuN) (Fig. 1). Most cells expressed the forebrain pyramidal cell markers MAP2, PAX6, and FoxG1. Identical to a previous report [16], the transcriptional factor FoxG1 is in the cytoplasm of differentiated neurons (Fig. 1). Positive staining indicates that the differentiation protocol converted hiPS and ES cells into neurons expressing specific forebrain markers.

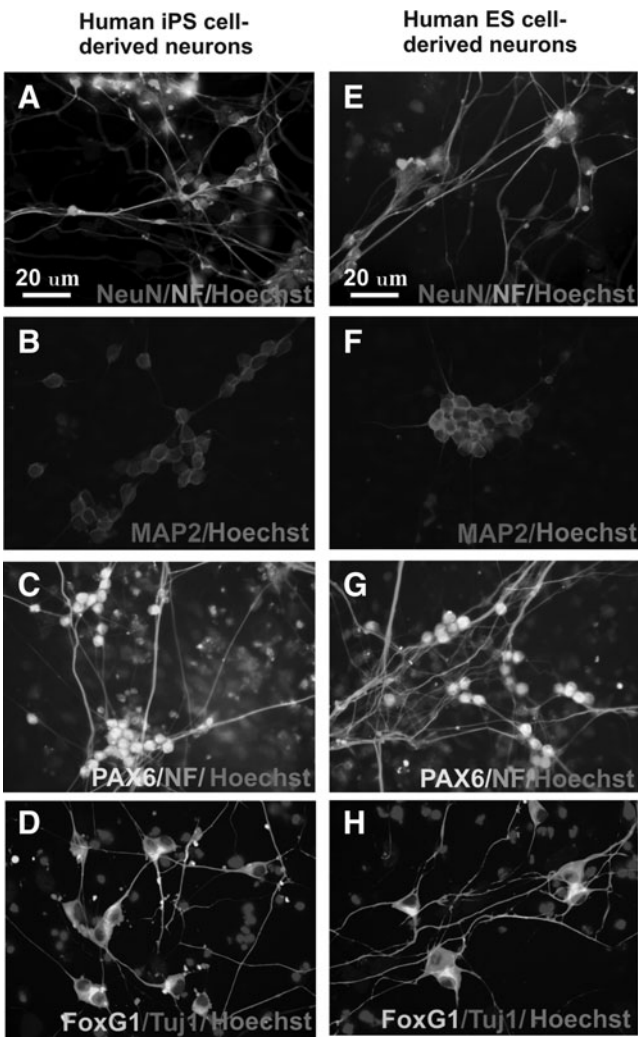

FIG. 1. Human induced pluripotent stem (hiPS) cell-derived neurons express forebrain pyramidal markers. After 4-week differentiation, hiPS cell-derived neurons show positive staining of NeuN and neurofilament (NF) **(A)**, microtubule-associated protein 2 (MAP2) **(B)**, paired box protein Pax-6 (PAX6) **(C)**, Tuj1, and forkhead box protein G1 (FoxG1) **(D)**. FoxG1 is located in the cytoplasm of differentiated neurons. In comparison, human ES cell-derived neurons also express the same neuronal markers NeuN, NF, MAP2, PAX6, Tuj1, and FoxG1 **(E–H)**.

Developmental changes of the RMPs and evoked APs

Over the 4-week differentiation and maturation of neural progenitor cells, we characterized the electrophysiological properties of these cells derived from hiPS and ES cells by measuring cell capacitance, RMP, and evoked APs. In whole-cell patch clamp recording of hiPS cell-derived

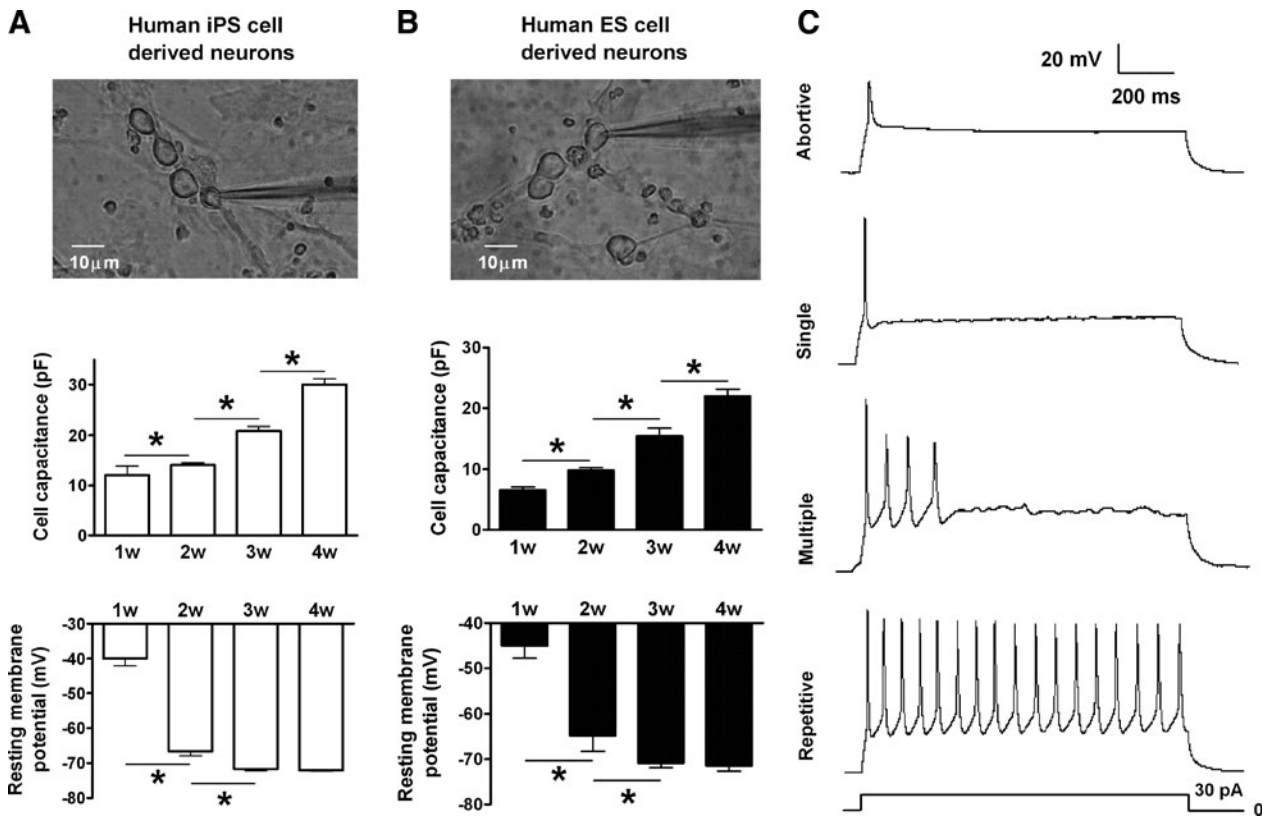

FIG. 2. Cell membrane capacitances, resting membrane potentials (RMPs), and action potential (AP) types in the differentiating neurons. **(A)** Whole-cell patch clamp recording of hiPS cell-derived neurons (*upper panel*) revealed a continuously increasing cell size (*middle panel*) and the development of cell RMPs from a depolarized to hyperpolarized level (*bottom panel*). **(B)** The same experiment and similar observations in human embryonic stem (ES) cell-derived neurons. **(C)** Abortive, single, and multiple, repetitive APs obtained in differentiating neurons derived from hiPS and ES cells. $^*P < 0.05$, comparing the correlated groups as indicated. $n = 6$–21 in each group.

neurons, the cell size determined by capacitance measurement progressively increased from an average of 12.0 ± 6.1 pF ($n = 10$) at week 1 to 30.1 ± 5.2 pF ($n = 18$ cells per groups; $P < 0.05$) by week 4 (Fig. 2A). The RMP steadily shifted from a relatively depolarized level of −40 mV in week 1 cells to the mature hyperpolarized level around −70 mV after 3- to 4-week differentiation (Fig. 2A). Human ES cell-derived neurons underwent the same developmental changes in cell capacitance and RMPs (Fig. 2B).

The ability to fire a train of repetitive APs upon membrane depolarization is a unique functional feature of mature neurons. To test the firing ability and firing pattern of differentiating cells, a 30 pA depolarization current of 1 s duration was injected into cells under whole-cell current clamp recording. For cells undergoing 1- to 4-week differentiation, we obtained 4 different firing types of APs (Fig. 2C and Table 1). These include (1) cells that fired abortive APs with a small amplitude and slow upstroke slope, (2) cells that fired only a single AP during the 1 s depolarization although the spike was large and sharp, (3) cells that fired <10 normal sharp APs, and (4) cells that fired repetitive normal APs over the 1 s depolarization (Fig. 2C). Importantly, the cells in the last group fired spikes without amplitude run-down. Early at week 1 of differentiation, all (100%) cells derived from hiPS and ES cells fired only abortive APs. At week 2, abortive APs disappeared and most of the cells (66.7% in hiPS cell cultures and 100% in human ES cell cultures) fired single APs (Table 2). At this time, some hiPS cell-derived neuron-like cells fired

Table 1. Four Types of APs Obtained in hiPS and ES Cell-Derived Neurons

AP type	*Peak amplitude (mV)*	*Upstroke slope (mV/ms)*	*½ AP width (ms)*	*Firing frequency (Hz)*
Abortive APs	38.78 ± 10.23$^{\#}$	6.03 ± 1.75$^{\#}$	11.71 ± 3.54*	1
Single APs	65.28 ± 7.86	18.49 ± 2.90	7.47 ± 1.03	1
Multiple APs	61.29 ± 5.36	14.93 ± 6.81	10.56 ± 4.76	4.00 ± 1.53
Repetitive APs	63.09 ± 3.26	22.59 ± 3.15§	6.16 ± 1.41§	15.44 ± 2.35

$^{\#}P < 0.01$, abortive APs compared to the 3 other AP types. $^*P < 0.01$, abortive APs compared to single and repetitive APs. $^{\S}P < 0.05$, repetitive APs compared to single and multiple APs. Mean ± SEM. $n = 16$–34 cells in each group.

APs, action potentials; iPS, induced pluripotent stem; ES, embryonic stem.

TABLE 2. FRACTION (%) OF HIPS AND ES CELL-DERIVED NEURONS EXPRESSING THE 4 TYPES OF APS IN EACH STAGE OF THE 4-WEEK DIFFERENTIATION

	Human iPS cells				*Human ES cells*			
AP types	1 w	2 w	3 w	4 w	1 w	2 w	3 w	4 w
Abortive APs	100	0	0	0	100	0	0	0
Single APs	0	66.7	54.5	22.2	0	100	72.2	58.8
Multiple APs	0	22.2	27.3	33.3	0	0	16.7	17.6
Repetitive APs	0	11.1	18.2	44.5	0	0	11.1	23.5

"w" stands for week.

multiple (22.2% of total) and repetitive APs (11.1% of total). At week 3, some human ES cells began to fire multiple (16.7%) and repetitive APs (11.1%). Meanwhile, 27.3% and 18.2% of iPS cell-derived neurons could fire multiple and repetitive APs, respectively. After 4-week differentiation, nearly half (44.5%) the iPS cell-derived neurons fired repetitive APs, while 23.5% of ES cell-derived neurons had a similar ability. These data suggest a progressive maturation of APs and functional development in hiPS cell-derived and ES cell-derived neurons.

Developmental changes of the inward Na^+ currents (I_{Na})

The amplitude of APs is determined by the population opening of voltage-gated Na^+ channels, we therefore characterized the developmental changes of I_{Na} over the 4-week neuronal differentiation. In hiPS cell-derived neurons at week 2 of differentiation, depolarizing voltage steps were applied in the presence of Cs^+, TEA, and Cd^{2+} in the bath solution to block voltage-gated K^+ and Ca^{2+} currents (Fig. 3A). The

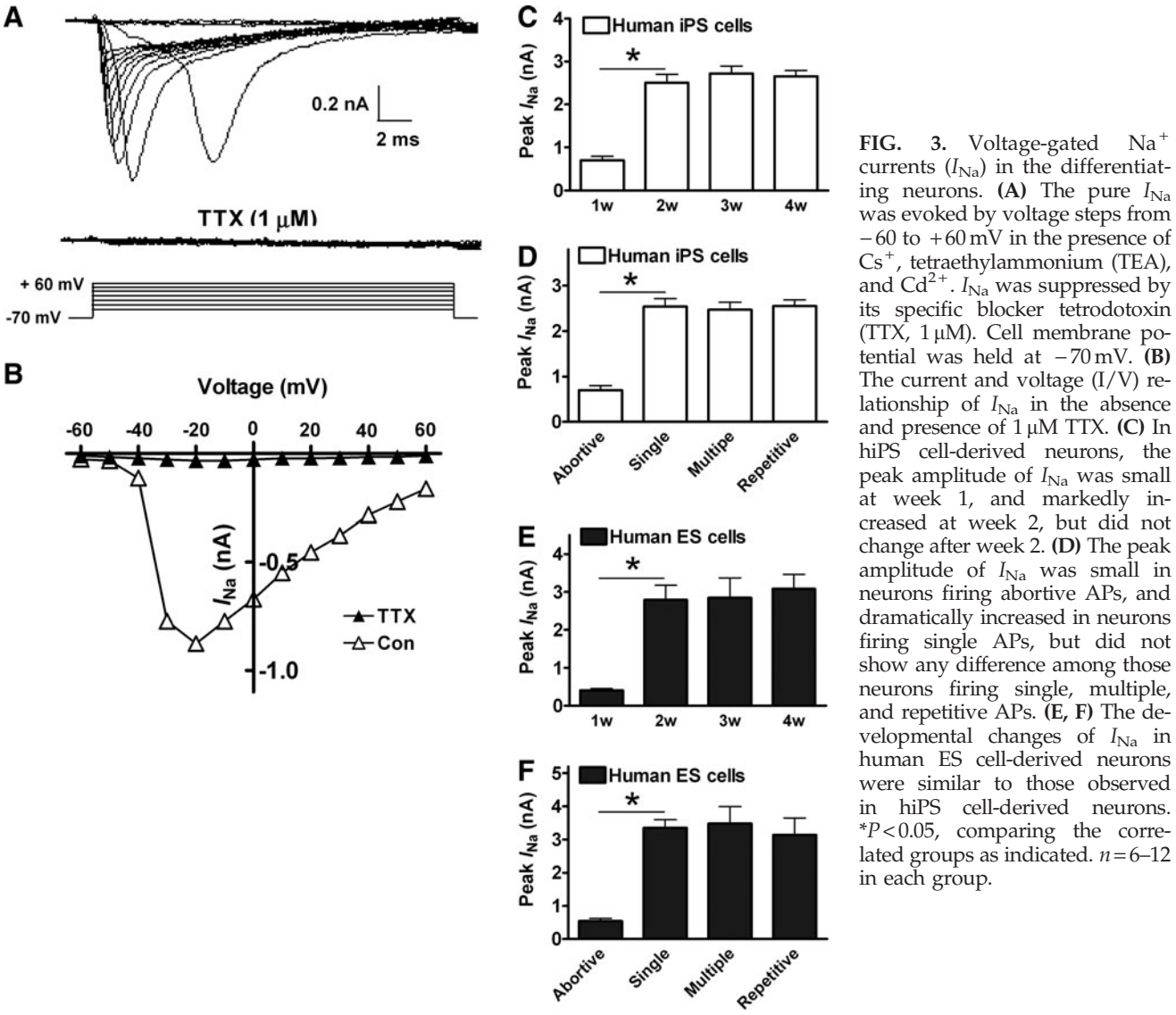

FIG. 3. Voltage-gated Na^+ currents (I_{Na}) in the differentiating neurons. **(A)** The pure I_{Na} was evoked by voltage steps from −60 to +60 mV in the presence of Cs^+, tetraethylammonium (TEA), and Cd^{2+}. I_{Na} was suppressed by its specific blocker tetrodotoxin (TTX, 1 μM). Cell membrane potential was held at −70 mV. **(B)** The current and voltage (I/V) relationship of I_{Na} in the absence and presence of 1 μM TTX. **(C)** In hiPS cell-derived neurons, the peak amplitude of I_{Na} was small at week 1, and markedly increased at week 2, but did not change after week 2. **(D)** The peak amplitude of I_{Na} was small in neurons firing abortive APs, and dramatically increased in neurons firing single APs, but did not show any difference among those neurons firing single, multiple, and repetitive APs. **(E, F)** The developmental changes of I_{Na} in human ES cell-derived neurons were similar to those observed in hiPS cell-derived neurons. *$P < 0.05$, comparing the correlated groups as indicated. $n = 6$–12 in each group.

evoked inward I_{Na} was confirmed by its sensitivity to the blocking action of 1 μM TTX and the current–voltage (I-V) relationship revealed by voltage steps from the holding potential of −70 mV up to +60 mV in 10 mV increments (Fig. 3B). In hiPS cell-derived neurons, the averaged amplitude of I_{Na} was small at week 1, and then markedly doubled in size at week 2, but did not show any significant difference at weeks 2, 3, and 4 (Fig. 3C). The averaged amplitude of I_{Na} was small in neurons firing abortive APs, while much larger I_{Na} was seen in neurons firing single, multiple, and repetitive APs (Fig. 3D). The same developmental change of I_{Na} was also observed in human ES-cell

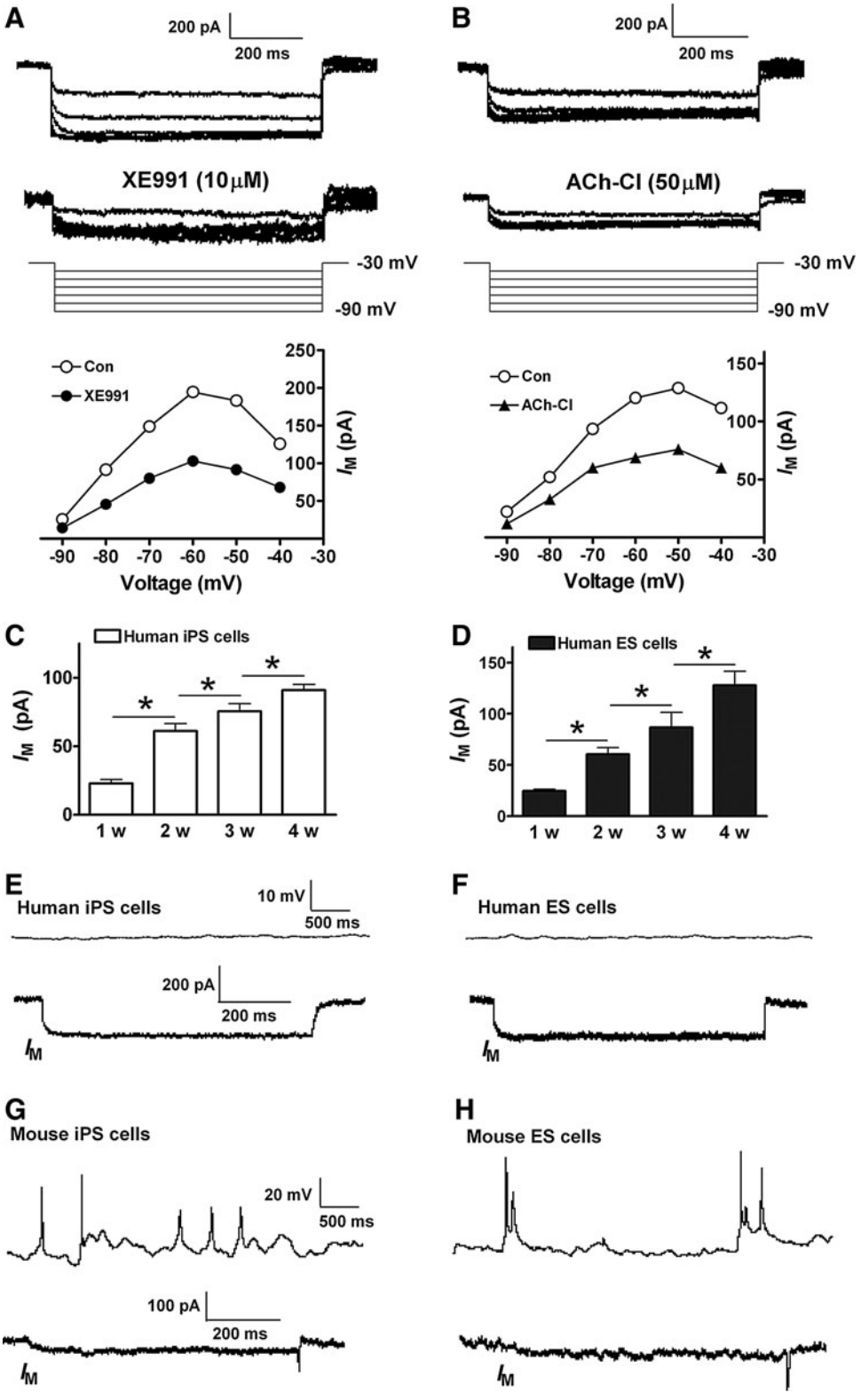

FIG. 4. M-currents (I_M) in the differentiating neurons. **(A)** Representative recordings of I_M in a 3-week neuron derived from hiPS cells. Cell membrane potential was held at −70 mV, I_M was activated by −30 mV prepulse in the presence of TTX (1 μM), and the deactivation of I_M was induced by voltage steps from −40 to −90 mV. XE991 (10 μM) was used to suppress I_M. **(B)** The deactivation of I_M was suppressed 20 min after bath application of Ach-Cl (50 μM). **(C, D)** show the time-dependent changes of I_M amplitude in hiPS and ES cell-derived neurons. HiPS and ES cell-derived mature neurons with substantial expression of I_M did not show spontaneous AP firing **(E, F)**. Mouse iPS and ES cell-derived neurons firing spontaneous APs showed very low expression of I_M **(G, H)**. $^*P < 0.05$, comparing the correlated groups as indicated. $n = 5$–11 in each group.

derived neurons over the 4-week cultures (Fig. 3E and 3F). This observation suggested that although a sufficient voltage-gated Na^+ channel activity was essential for firing a normal AP, the firing pattern of APs was not determined by the amplitude of Na^+ currents.

M-type K^+ currents (I_M) during neuronal differentiation

The M-current (I_M) controls the excitability of neurons via maintaining the membrane potential below the threshold for the activation of voltage-gated Na^+ channels [10]. We next characterized I_M in the hiPS and ES cell-derived neurons during the 4-week neuronal differentiation. In whole-cell recording, cells were held at −70 mV and a −30 mV prepulse was used to activate I_M, followed by deactivation of hyperpolarizing pulses from −40 to −90 mV in the presence of TTX (1 μM). The size of I_M was determined by measuring the amplitude of the deactivation current upon a 20-mV hyperpolarization step (from −30 to −50 mV). The current was sensitive to the inhibitory action of the I_M blocker 10,10-bis(4-pyridinylmethyl)-9(10H)-anthracenone (XE991) (Fig. 4A). We also tested the inhibitory effect of bath applied muscarinic receptor agonist acetylcholine chloride (ACh-Cl) on the current (Fig. 4B). After 1 week into neuronal differentiation, the amplitude of I_M was small in hiPS cell-derived neurons. The current then gradually increased over the ensuing 2–4-week differentiation period (Fig. 4C). The same developmental change of I_M was also observed in human ES cell-derived neurons (Fig. 4D). One important action of I_M is to suppress spontaneous AP firing in mature neurons. Consistently, whole-cell current clamp recordings showed that very few spontaneous APs were observed in hiPS and ES cell-derived neurons at the ages of 3–4-week differentiation (Fig. 4E and 4F). This low-spontaneous activity likely results from the robust activity of I_M in these cells. Supporting this speculation, in mouse iPS and ES cell-derived neurons differentiated for 8–10 days, the amplitude of I_M was very low and a much higher percentage of the neuron-like cells (~50% of total) showed spontaneous firing of APs (Fig. 4G and H).

Delayed rectifier (I_K) and transient A-type (I_A) K^+ currents in the developing neurons

The delayed rectifier I_K and the fast inactivating I_A currents are 2 other K^+ currents that can control the firing pattern of APs via repolarizing the membrane potential during and soon after APs. In whole-cell recordings on hiPS cell-derived neuron-like cells, the cell membrane potential was held at −70 mV, and I_K was elicited by voltage commands from −60 to +60 mV with 20 mV increments in the presence of TTX (1 μM) and Cd^{2+} (100 μM). The currents showed a relatively slow activating and inactivating property upon the on and off phase of the voltage command. The current kinetics and its sensitivity to TEA block were consistent with a delayed rectifier current (Fig. 5A). I_K could be recorded in all examined cells undergoing 1- to 4-week differentiation. On the other hand, the transient I_A current was commonly seen only in cells during the late stages (3–4 weeks) of neuronal differentiation. After a hyperpolarizing prepulse of −110 mV, I_A was elicited by voltage steps from −60 to

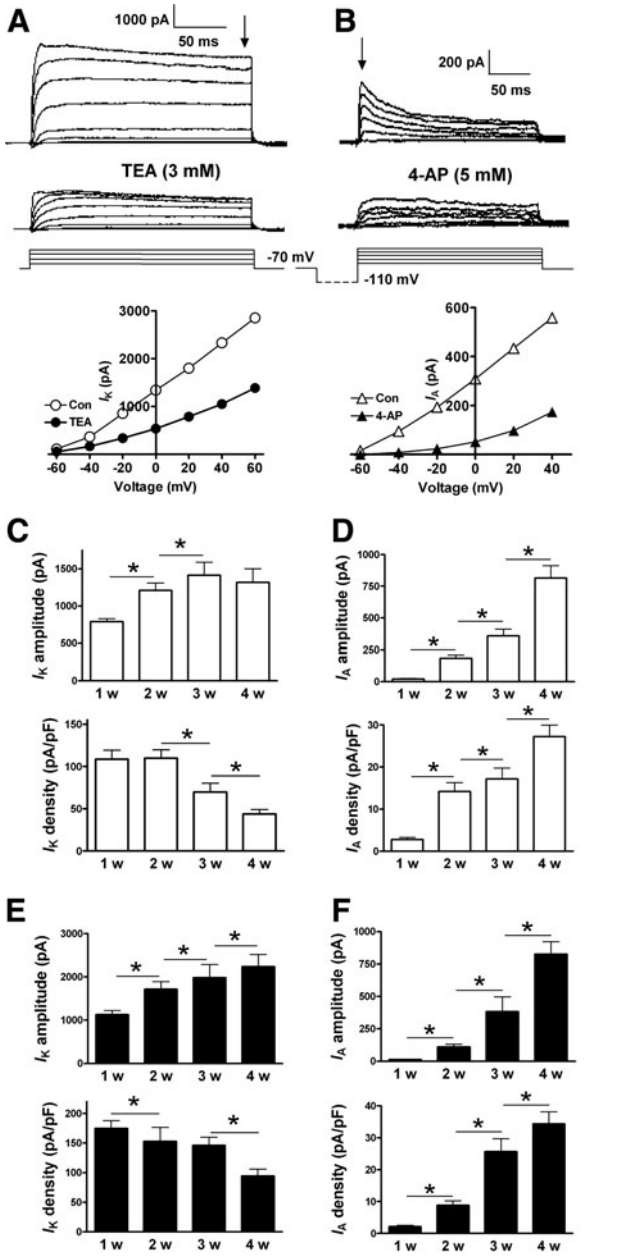

FIG. 5. Delayed rectifier (I_K) and transient A-type (I_A) K^+ currents in the developing neurons. **(A)** I_K was elicited by voltage steps from −60 to +60 mV with a 20-mV step in the presence of TTX (1 μM) and Cd^{2+} (100 μM) with holding potential at −70 mV. The amplitude of I_K was measured at the end of a +40-mV voltage command (indicated by the *vertical arrow*). *Bottom panel* shows the I/V relationship curve of I_K in the presence and absence of 3 mM TEA. **(B)** I_A was elicited by voltage steps from −60 to +60 mV with 20 mV increment, following a hyperpolarization pulse of −110 mV. The amplitude of I_A was determined by measuring the size of the peak component (indicated by the *vertical arrow*). *Bottom panel* shows the I/V relationship curve of I_A before and after the application of 4-aminopyridine (4-AP) (5 mM). **(C)** I_K amplitude and density in differentiating neurons derived from hiPS cells. **(D)** Time-dependent increase of I_A in differentiating neurons derived from hiPS cells. **(E, F)** Amplitude and density of I_K and I_A currents in the differentiating neurons derived from human ES cells. *$P < 0.05$, comparing the correlated groups as indicated. $n = 7$–14 in each group.

+60 mV with 20 mV increments. Different from the sustained I_K current, I_A displayed fast activating and inactivating kinetics. The peak I_A current was suppressed by bath application of 4-aminopyridine (4-AP) (Fig. 5B).

We next analyzed the amplitude of I_K and I_A in these cells along the 4-week differentiation. In hiPS cell-derived neuron-like cells, the averaged size of I_K gradually increased from 1 to 3 weeks, and then remained unchanged at week 4 (Fig. 5C). Because the cell size underwent continuous increase over the 4-week differentiation, we calculated the current density of I_K and observed no difference in the I_K current density between week 1 and 2. The current density, however, was significantly decreased over the ensuing weeks 3 and 4 (Fig. 5C). On the other hand, the transient I_A current was rarely obtained at week 1. In the following weeks, I_A showed a dramatic increase in amplitude as well as in its current density (Fig. 5D). Similar developmental changes in the I_K and I_A amplitude and current density were also observed in human ES cell-derived neuronal cells (Fig. 5E, 5F).

Increased I_A currents played a major role in regulating the firing pattern of APs in differentiated neurons

Functional expression of transient I_A channels was almost absent in immature neurons firing abortive and single APs (Fig. 6A, 6B and 6E) and large I_A currents were regularly seen in mature neurons that fired multiple and repetitive APs (Fig. 6C, 6D and 6E). Similar changes were found in human ES cell-derived neurons (Fig. 6F). These data suggest that the transient current I_A rather than the sustained current I_K plays an important role in shaping the AP firing pattern. Supporting this idea, blocking the I_A current using 4-AP (5 mM) in neurons firing repetitive APs effectively reduced the AP firing frequency and elongated the half width of APs (Fig. 7A, 7B).

The experimental evidences from mouse iPS and ES cells also support this conclusion. Mouse iPS and ES cell-derived neuroepithelial cells differentiated into mature neurons within 8–10 days. The sustained K^+ current I_K was present in all mouse iPS and ES cell-derived neurons expressing single and

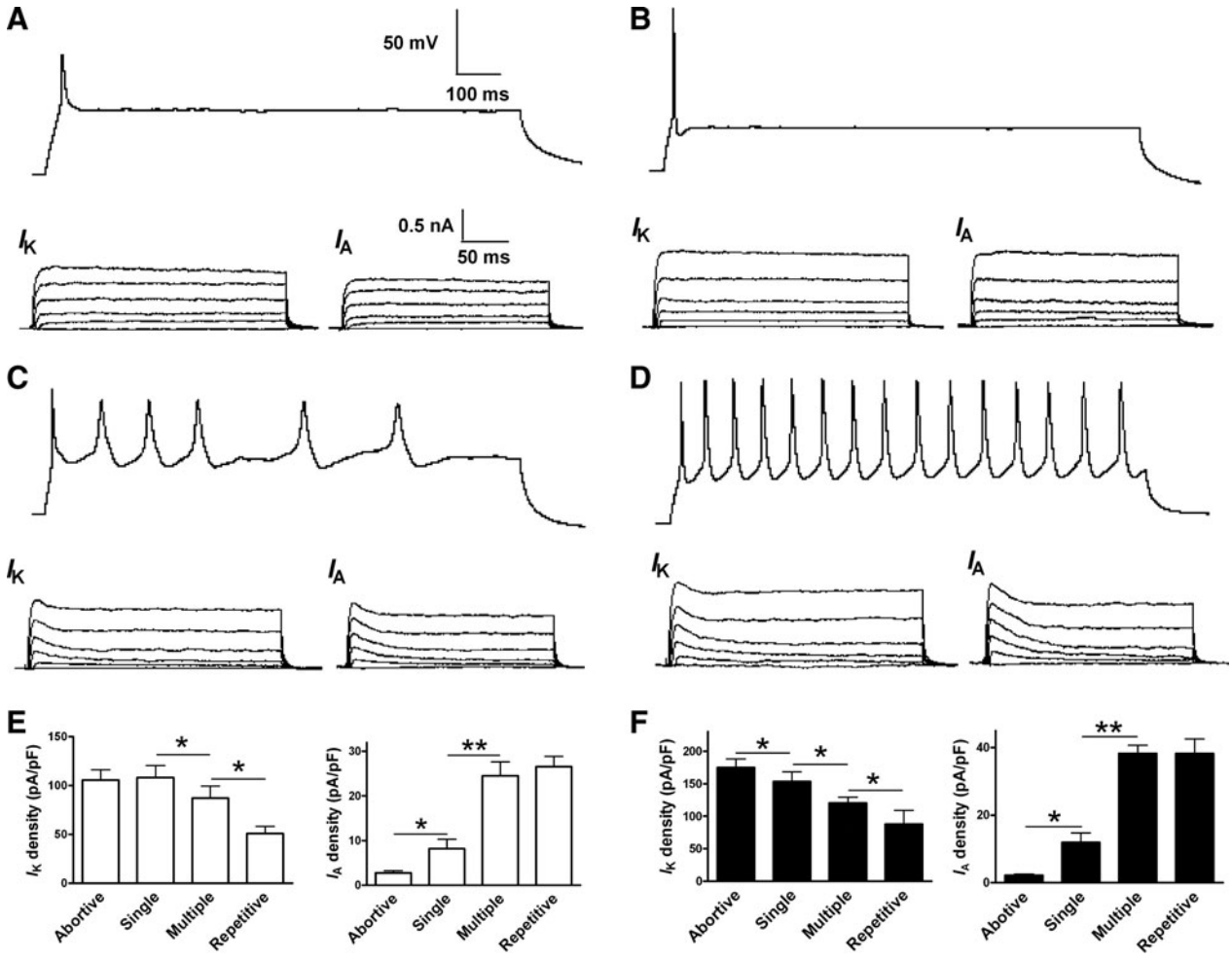

FIG. 6. I_K and I_A in hiPS and ES cell-derived neurons. I_K and I_A were recorded in neuron-like cells firing abortive, single, multiple, and repetitive APs. **(A, B)** I_K and very tiny I_A can be recorded in hiPS cell-derived neurons firing abortive and single APs. I_K and I_A were evoked and measured as described in Fig. 5. **(C, D)** Both I_K and I_A (indicated by their peak component) can be substantially obtained in mature neurons able to fire multiple and repetitive APs. **(E)** Current density of I_K and I_A in hiPS cell-derived neurons firing different APs. **(F)** Current density of I_K and I_A in human ES cell-derived neurons firing different APs. $^*P < 0.05$; $^{**}P < 0.01$, comparing the correlated groups as indicated. $n = 5$–12 in each group.

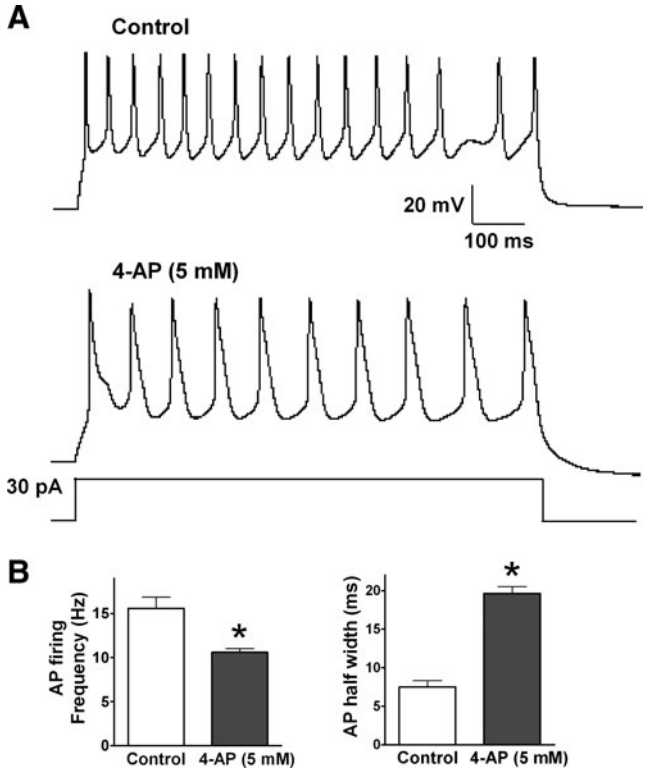

FIG. 7. The effect of I_A channel blocker 4-AP on AP firing pattern. **(A)** The morphology of repetitive APs recorded in hiPS cell-derived neurons (*upper*) is shaped by the application of 5 mM 4-AP (*lower*). **(B)** 4-AP (5 mM) decreases the firing frequency of repetitive APs (*left*), but greatly increases their half widths (*right*). $^*P < 0.05$, comparing the correlated groups as indicated. $n = 5$ in each group.

multiple APs. The current density of I_K did not show significant differences between neurons firing single and multiple APs. In those neurons firing a single AP, the transient current I_A was very small (Fig. 8A and 8B). In neurons firing multiple APs, the I_A current markedly increased (Fig. 8C and 8D). The current density of I_A in neurons expressing multiple APs was much higher than those with a single AP (Fig. 8E and 8F).

Voltage-gated Ca^{2+} currents and spontaneous synaptic activity in the developing neurons

Ca^{2+} plays important roles in a variety of signal transduction pathways and neuronal functions. The typical role of Ca^{2+} entry is to trigger the release of neurotransmitters from the presynapse into the synaptic cleft. In our study, 100 μM $CdCl_2$ was used to block voltage-gated Ca^{2+} channels when voltage-gated Na^+ and K^+ currents were recorded. To record HVA Ca^{2+} currents, cells were held at −70 mV, and then a series of voltage steps from −60 to +60 mV in 20 mV increments were applied in the presence of TTX, Cs^+, and TEA. In hiPS cell-derived neurons, $CdCl_2$-sensitive HVA Ca^{2+} currents were observed (Fig. 9A and 9B). The HVA Ca^{2+} currents were low at week 1, and then gradually increased over the following weeks (Fig. 9C). The expression of HVA Ca^{2+} currents in human ES cell-derived neurons also underwent the same developmental changes over the 4-week differentiation (Fig. 9D).

Spontaneous neurotransmitter release occurs in the absence of APs and usually can be obtained in the presence of TTX. To detect the synaptic function of the developing neurons, we recorded miniature excitatory postsynaptic currents (mEPSCs) at a holding potential of −80 mV in hiPS and ES cell-derived neurons. mEPSCs showed inward currents and were suppressed by the α-amino-3-hydroxy-5-methyl-4-isoxazolepropionic acid (AMPA) receptor antagonist NBQX (20 μM) (Fig. 9E). The miniature inhibitory postsynaptic currents (mIPSCs) were recorded at a holding potential of 0 mV. This depolarizing command lead to a fluctuation in cell membrane potentials, but we could still record and suppress the outward mIPSCs by using the gamma-aminobutyric acid (GABA) receptor antagonist bicuculline (50 μM) (Fig. 9E). Both mEPSCs and mIPSCs can be observed throughout the 4-week differentiation of hiPS and ES cells.

Discussion

In the present investigation, we characterized the developmental changes in the electrophysiological features of neuron-like cells derived from hiPS and ES cells. After the 4-week terminal differentiation, these cells stably express specific forebrain pyramidal neuronal makers, including NeuN, NF, MAP2, Tuj1, PAX6, and FoxG1. Over the period of differentiation, the cell size increased continuously and the RMP showed a negative shift toward −70 mV. We identified that I_M contributes to the development of cell RMPs and neuronal excitability. The firing patterns of APs were progressively converted from the abortive to the repetitive type, and the size of sharp APs increased with maturation of differentiated neurons. Interestingly, we noticed that the developmental changes in the amplitude of I_{Na} did not correlate with the firing patterns of APs. The transient A-type K^+ current I_A rather than the sustained current I_K was a key regulator for the functional activity of maturing APs. The functional synaptic activity indicated by the spontaneous miniature potentials could be observed in the developing neurons from 1 to 4 weeks.

The neuronal proteins NeuN, NF, and Tuj1 are expressed in most neuronal cells in the nervous system, including the forebrain in vertebrates. NeuN immunoreactivity is extensively used to identify neuronal cells during development and in adult and neurological diseases [17,18]. The NF protein is the major intermediate filament involved in axon growth and stabilization of the axonal cytoskeleton [19,20]. Tuj1 is an important neuronal marker specific for developing and maturing neurons [21]. In the postnatal forebrain, most neurons originate from those Tuj1-positive progenitor cells in the anterior part of the subventricular zone [22,23]. The neuronal cells derived from hiPS and ES cells in this investigation also express MAP2, PAX6, and FoxG1. MAP2 is a forebrain pyramidal cell marker, mainly expressed on dendrites of pyramidal neurons in the cerebral cortex and hippocampus [24,25]. PAX6 is a transcription factor involved in nervous system development [26]. Associated with other transcription factors, PAX6 plays a critical role in determining the fate of neuronal progenitors and controlling the density of cortical neurons in the developing forebrain [27–29]. PAX6 is also used as a pyramidal cell marker based on its indispensable role in the neurogenesis of pyramidal neurons in the forebrain [30,31]. The transcription factor FoxG1 expressed in

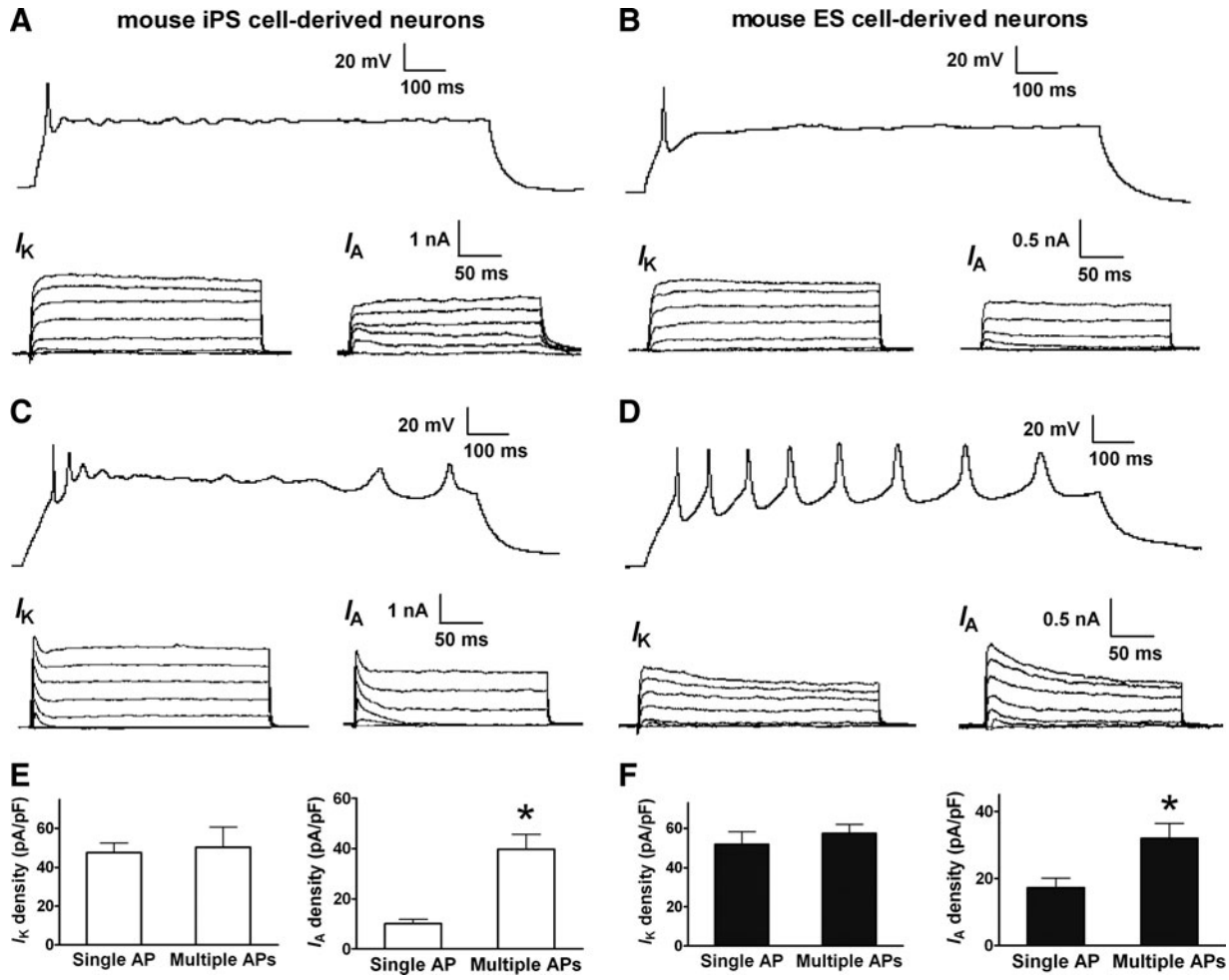

FIG. 8. K^+ channel activities in mouse stem cell-derived neurons. I_K and I_A in mouse iPS and ES cell-derived neurons firing single and multiple APs. **(A, B)** I_K and very small I_A can be recorded in mouse iPS and ES cell-derived neurons firing single APs. I_K and I_A were evoked and measured as described in Fig. 5. **(C, D)** Both I_K and I_A (indicated by their peak component) can be substantially obtained in mouse neurons able to fire multiple APs. **(E)** Current density of I_K and I_A in mouse iPS cell-derived neurons firing different APs. **(F)** Current density of I_K and I_A in mouse ES cell-derived neurons firing different APs. $^*P < 0.05$, comparing the correlated groups as indicated. $n = 4$–12 in each group.

the forebrain plays an important role in cortical development by regulating progenitor proliferation and neurogenesis [32]. The FoxG1 protein is localized in the nucleus of neuronal progenitors and relocated into the cytoplasm after differentiation [16]. In the intermediate zone of the cortex, dynamic expression of FoxG1 is an essential mechanism for migration of pyramidal neuron progenitors into the cerebral cortex [33]. These histological evidences of positive staining of NeuN, NF, Tuj1, MAP2, PAX6, and FoxG1 strongly indicate that our differentiation method has converted hiPS and ES cells into forebrain pyramidal-like neurons.

The developmental changes in these electrophysiological characters were very similar between iPS cell- and ES cell-derived progenitors and neuron-like cells. The electrophysiological properties of developing neurons derived from hiPS and ES cells also mimic the physiologic maturation of pyramidal neurons in the animal neocortex after birth [34–39]. During the development of the animal neocortex, pyramidal neuron RMPs become more negative, the duration of APs is shortening, and their firing pattern is converted from single to repetitive firing. Meanwhile, the voltage-dependent Na^+, K^+, and Ca^{2+} currents undergo specific time-dependent changes [34–39]. Our observation demonstrates that hiPS cells generated from adult cells are capable of differentiating into functional brain neurons via similar physiological processes as those of ES cells.

For neurons, the typical feature of electrophysiological maturation is the ability to fire trains of repetitive sharp APs in response to depolarizing current injection. Immature neurons derived from hiPS and ES cells only showed abortive APs at week 1, most likely resulting from the low expression of I_{Na} assessed by the peak amplitude measurement. At week 2, most of the cells fired a large single AP, and the peak amplitude of I_{Na} also dramatically increased. When the differentiation entered weeks 3 and 4, maturing neurons were able to fire multiple and repetitive APs. We did not observe a significant amplitude difference among the single, multiple, and repetitive APs, and the averaged amplitude of I_{Na} did not show any difference among the neurons firing single, multiple, and repetitive APs. Thus, I_{Na} plays a

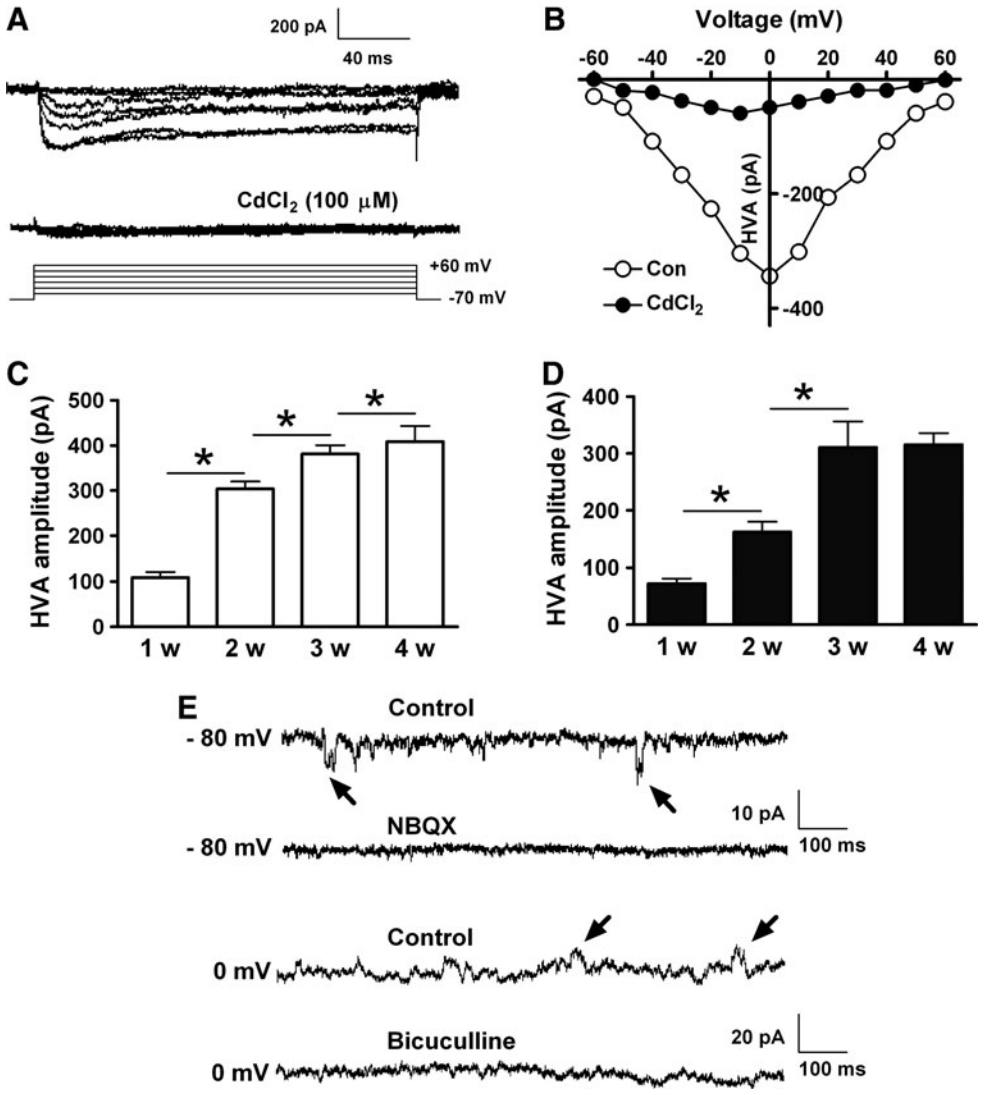

FIG. 9. Voltage-gated Ca^{2+} currents and spontaneous synaptic activity in the developing neurons. **(A)** In a 3-week hiPS cell-derived neuron, the high-voltage-activated (HVA) Ca^{2+} currents were evoked by voltage steps from −60 to +60 mV in presence of TTX, Cs^+, and TEA. 100 μM $CdCl_2$ was used to inhibit HVA Ca^{2+} currents. **(B)** The I/V relationship curve of HVA Ca^{2+} currents before and after application of $CdCl_2$. **(C)** The amplitude of HVA Ca^{2+} currents in differentiating neurons derived from hiPS cells. **(D)** HVA Ca^{2+} currents in differentiating neurons derived from human ES cells. **(E)** Miniature excitatory and inhibitory postsynaptic currents (mE/IPSCs) were recorded at holding potentials of −80 and 0 mV, respectively. α-amino-3-hydroxy-5-methyl-4-isoxazolepropionic acid (AMPA) receptor antagonist NBQX (20 μM) and gamma-aminobutyric acid (GABA) receptor antagonist bicuculline (50 μM) were used to suppress mE/IPSCs. $^*P < 0.05$, comparing the correlated groups as indicated. $n = 5$–8 in each group.

dominant role in the AP amplitude as described in previous reports [40], but not in the evolution of AP firing patterns.

The functional expression of the transient outward K^+ current I_A plays an imperative role in neuronal maturation leading to repetitive AP firing. The current density of I_A markedly increased in a time- and differentiation-dependent manner despite the growing cell size during the 4-week development. This coincides well with the progressively increased ability of cells to fire repetitive APs. Additionally, we show that, in mature neurons, blocking I_A effectively reduced the number of APs and increased their half widths. Thus, the temporal expression of I_A and its regulation of AP firing patterns in iPS cell-derived pyramidal neurons mimic the same mechanism seen in developing cortical neurons and neurons from human ES cells [11,12,41,42]. In animal pyramidal neurons, I_A channels are assembled from α–subunits of the K_v4 and K_v1 family, while I_K channels are composed of K_v2 subunits [43–45]. The function and the molecular subunits composition of voltage-gated K^+ channels differ greatly in different brain regions and neuronal types. In the hippocampal interneurons and basal ganglia output neurons, I_K is encoded by the K_v3 subunit family and required for sustained high-frequency AP generation [46,47]. The contribution of I_A rather than I_K to AP maturation in hiPS cell-derived neurons fits well with that discovered in neocortical pyramidal neurons.

Our data also show a time-dependent increase of voltage-gated Ca^{2+} currents in differentiating cells. The HVA Ca^{2+} channels mediate a rapid Ca^{2+} entry that triggers AP-evoked neurotransmitter releases [48,49]. This Ca^{2+} entry, however, is not required for the spontaneous transmitter release in the absence of APs [50,51]. The spontaneous miniature postsynatpic potentials could be obtained in the differentiating cells at the early age of week 1, suggesting that the onset of the synaptic activity appears much earlier than AP generation and neuronal maturation.

Taken together, the present study provides a compelling new evidence to show that hiPS cells, like human ES cells, can be converted into functional pyramidal-like neurons. Our feeder-free neuronal differentiation protocol helps neural progenitors quickly become maturing neurons in 4 weeks. Temporal coordination between voltage-gated Na^+ and K^+ currents controls functional maturation of these neurons. The morphological features and electrophysiological properties of hiPS cell-derived neurons are very similar to those found in human ES cell-derived neurons. Thus, hiPS cells generated

from adult somatic cells maintain the intrinsic properties of human ES cells and are able to form functional neurons. The confirmation of these properties in other hiPS cell lines is important for the development of cell-based therapies using hiPS cells.

Acknowledgment

This work was supported by the NIH grants NS0458710 (SPY), American Heart Association (AHA) Grant-in-Aid 12GRNT12060222 (SPY), and AHA Postdoctoral Fellowship 12POST12080252 (MS). This work was also supported by the NIH grant C06 RR015455 from the Extramural Research Facilities Program of the National Center for Research Resources.

Author Disclosure Statement

There is no commercial association involved in this investigation and no conflict of interests in connection with any author in the submitted manuscripts. No competing financial interests exist in this investigation.

References

1. Fischbach GD and RL Fischbach. (2004). Stem cells: science, policy, and ethics. J Clin Invest 114:1364–1370.
2. Takahashi K, K Tanabe, M Ohnuki, M Narita, T Ichisaka, K Tomoda and S Yamanaka. (2007). Induction of pluripotent stem cells from adult human fibroblasts by defined factors. Cell 131:861–872.
3. Hu BY, JP Weick, J Yu, LX Ma, XQ Zhang, JA Thomson and SC Zhang. (2010). Neural differentiation of human induced pluripotent stem cells follows developmental principles but with variable potency. Proc Natl Acad Sci U S A 107:4335–4340.
4. Chen X and D Johnston. (2004). Properties of single voltage-dependent K+ channels in dendrites of CA1 pyramidal neurones of rat hippocampus. J Physiol 559:187–203.
5. Storm JF. (1990). Potassium currents in hippocampal pyramidal cells. Prog Brain Res 83:161–187.
6. Bossu JL, M Capogna, D Debanne, RA McKinney and BH Gahwiler. (1996). Somatic voltage-gated potassium currents of rat hippocampal pyramidal cells in organotypic slice cultures. J Physiol 495 (Pt 2):367–381.
7. Staff NP, HY Jung, T Thiagarajan, M Yao and N Spruston. (2000). Resting and active properties of pyramidal neurons in subiculum and CA1 of rat hippocampus. J Neurophysiol 84:2398–2408.
8. Tyzio R, A Ivanov, C Bernard, GL Holmes, Y Ben-Ari and R Khazipov. (2003). Membrane potential of CA3 hippocampal pyramidal cells during postnatal development. J Neurophysiol 90:2964–2972.
9. Bean BP. (2007). The action potential in mammalian central neurons. Nat Rev Neurosci 8:451–465.
10. Delmas P and DA Brown. (2005). Pathways modulating neural KCNQ/M (Kv7) potassium channels. Nat Rev Neurosci 6:850–862.
11. Kim J, DS Wei and DA Hoffman. (2005). Kv4 potassium channel subunits control action potential repolarization and frequency-dependent broadening in rat hippocampal CA1 pyramidal neurones. J Physiol 569:41–57.
12. Mitterdorfer J and BP Bean. (2002). Potassium currents during the action potential of hippocampal CA3 neurons. J Neurosci 22:10106–10115.
13. Chambers SM, CA Fasano, EP Papapetrou, M Tomishima, M Sadelain and L Studer. (2009). Highly efficient neural conversion of human ES and iPS cells by dual inhibition of SMAD signaling. Nat Biotechnol 27:275–280.
14. Drury-Stewart D, M Song, O Mohamad, SP Yu and Wei L. (2012). Small molecule promoted feeder free and adherent differentiation of functional neurons from human embryonic and induced pluripotent stem cells. J Stem Cells 6:1–8.
15. Cui L, J Jiang, L Wei, X Zhou, JL Fraser, BJ Snider and SP Yu. (2008). Transplantation of embryonic stem cells improves nerve repair and functional recovery after severe sciatic nerve axotomy in rats. Stem Cells 26:1356–1365.
16. Regad T, M Roth, N Bredenkamp, N Illing and N Papalopulu. (2007). The neural progenitor-specifying activity of FoxG1 is antagonistically regulated by CKI and FGF. Nat Cell Biol 9:531–540.
17. Mullen RJ, CR Buck and AM Smith. (1992). NeuN, a neuronal specific nuclear protein in vertebrates. Development 116:201–211.
18. Wolf HK, R Buslei, R Schmidt-Kastner, PK Schmidt-Kastner, T Pietsch, OD Wiestler and I Blumcke. (1996). NeuN: a useful neuronal marker for diagnostic histopathology. J Histochem Cytochem 44:1167–1171.
19. Shea TB and ML Beermann. (1994). Respective roles of neurofilaments, microtubules, MAP1B, and tau in neurite outgrowth and stabilization. Mol Biol Cell 5:863–875.
20. Lee MK and DW Cleveland. (1994). Neurofilament function and dysfunction: involvement in axonal growth and neuronal disease. Curr Opin Cell Biol 6:34–40.
21. Menezes JR and MB Luskin. (1994). Expression of neuron-specific tubulin defines a novel population in the proliferative layers of the developing telencephalon. J Neurosci 14: 5399–5416.
22. Menezes JR, CM Smith, KC Nelson and MB Luskin. (1995). The division of neuronal progenitor cells during migration in the neonatal mammalian forebrain. Mol Cell Neurosci 6:496–508.
23. Luskin MB, T Zigova, BJ Soteres and RR Stewart. (1997). Neuronal progenitor cells derived from the anterior subventricular zone of the neonatal rat forebrain continue to proliferate in vitro and express a neuronal phenotype. Mol Cell Neurosci 8:351–366.
24. Curtetti R, D Garbossa and A Vercelli. (2002). Development of dendritic bundles of pyramidal neurons in the rat visual cortex. Mech Ageing Dev 123:473–479.
25. Hayashi N, A Oohira and S Miyata. (2005). Synaptic localization of receptor-type protein tyrosine phosphatase zeta/beta in the cerebral and hippocampal neurons of adult rats. Brain Res 1050:163–169.
26. Mastick GS and GL Andrews. (2001). Pax6 regulates the identity of embryonic diencephalic neurons. Mol Cell Neurosci 17:190–207.
27. Jones L, G Lopez-Bendito, P Gruss, A Stoykova and Z Molnar. (2002). Pax6 is required for the normal development of the forebrain axonal connections. Development 129:5041–5052.
28. Englund C, A Fink, C Lau, D Pham, RA Daza, A Bulfone, T Kowalczyk and RF Hevner. (2005). Pax6, Tbr2, and Tbr1 are expressed sequentially by radial glia, intermediate progenitor cells, and postmitotic neurons in developing neocortex. J Neurosci 25:247–251.
29. Quinn JC, M Molinek, BS Martynoga, PA Zaki, A Faedo, A Bulfone, RF Hevner, JD West and DJ Price. (2007). Pax6 controls cerebral cortical cell number by regulating exit from

the cell cycle and specifies cortical cell identity by a cell autonomous mechanism. Dev Biol 302:50–65.
30. Hevner RF, RD Hodge, RA Daza and C Englund. (2006). Transcription factors in glutamatergic neurogenesis: conserved programs in neocortex, cerebellum, and adult hippocampus. Neurosci Res 55:223–233.
31. Maekawa M, N Takashima, Y Arai, T Nomura, K Inokuchi, S Yuasa and N Osumi. (2005). Pax6 is required for production and maintenance of progenitor cells in postnatal hippocampal neurogenesis. Genes Cells 10:1001–1014.
32. Martynoga B, H Morrison, DJ Price and JO Mason. (2005). Foxg1 is required for specification of ventral telencephalon and region-specific regulation of dorsal telencephalic precursor proliferation and apoptosis. Dev Biol 283:113–127.
33. Miyoshi G and G Fishell. (2012). Dynamic FoxG1 expression coordinates the integration of multipolar pyramidal neuron precursors into the cortical plate. Neuron 74:1045–1058.
34. McCormick DA and DA Prince. (1987). Post-natal development of electrophysiological properties of rat cerebral cortical pyramidal neurones. J Physiol 393:743–762.
35. Huguenard JR, OP Hamill and DA Prince. (1988). Developmental changes in Na+ conductances in rat neocortical neurons: appearance of a slowly inactivating component. J Neurophysiol 59:778–795.
36. Beique JC, B Campbell, P Perring, MW Hamblin, P Walker, L Mladenovic and R Andrade. (2004). Serotonergic regulation of membrane potential in developing rat prefrontal cortex: coordinated expression of 5-hydroxytryptamine (5-HT)1A, 5-HT2A, and 5-HT7 receptors. J Neurosci 24:4807–4817.
37. Zhang ZW. (2004). Maturation of layer V pyramidal neurons in the rat prefrontal cortex: intrinsic properties and synaptic function. J Neurophysiol 91:1171–1182.
38. Higgs MH and WJ Spain. (2009). Conditional bursting enhances resonant firing in neocortical layer 2–3 pyramidal neurons. J Neurosci 29:1285–1299.
39. Guan D, LR Horton, WE Armstrong and RC Foehring. (2011). Postnatal development of A-type and Kv1- and Kv2-mediated potassium channel currents in neocortical pyramidal neurons. J Neurophysiol 105:2976–2988.
40. Hodgkin AL and AF Huxley. (1952). Currents carried by sodium and potassium ions through the membrane of the giant axon of Loligo. J Physiol 116:449–472.
41. Johnson MA, JP Weick, RA Pearce and SC Zhang. (2007). Functional neural development from human embryonic stem cells: accelerated synaptic activity via astrocyte coculture. J Neurosci 27:3069–3077.
42. Yuan W, A Burkhalter and JM Nerbonne. (2005). Functional role of the fast transient outward K+ current IA in pyramidal neurons in (rat) primary visual cortex. J Neurosci 25:9185–9194.
43. Nerbonne JM, BR Gerber, A Norris and A Burkhalter. (2008). Electrical remodelling maintains firing properties in cortical pyramidal neurons lacking KCND2-encoded A-type K+ currents. J Physiol 586:1565–1579.
44. Kihira Y, TO Hermanstyne and H Misonou. (2010). Formation of heteromeric Kv2 channels in mammalian brain neurons. J Biol Chem 285:15048–15055.
45. Norris AJ and JM Nerbonne. (2010). Molecular dissection of I(A) in cortical pyramidal neurons reveals three distinct components encoded by Kv4.2, Kv4.3, and Kv1.4 alpha-subunits. J Neurosci 30:5092–5101.
46. Lien CC and P Jonas. (2003). Kv3 potassium conductance is necessary and kinetically optimized for high-frequency action potential generation in hippocampal interneurons. J Neurosci 23:2058–2068.
47. Ding S, SG Matta and FM Zhou. (2011). Kv3-like potassium channels are required for sustained high-frequency firing in basal ganglia output neurons. J Neurophysiol 105:554–570.
48. DeLorenzo RJ, SD Freedman, WB Yohe and SC Maurer. (1979). Stimulation of Ca2+-dependent neurotransmitter release and presynaptic nerve terminal protein phosphorylation by calmodulin and a calmodulin-like protein isolated from synaptic vesicles. Proc Natl Acad Sci U S A 76:1838–1842.
49. Littleton JT, M Stern, M Perin and HJ Bellen. (1994). Calcium dependence of neurotransmitter release and rate of spontaneous vesicle fusions are altered in Drosophila synaptotagmin mutants. Proc Natl Acad Sci U S A 91:10888–10892.
50. Glitsch MD. (2008). Spontaneous neurotransmitter release and Ca2+—how spontaneous is spontaneous neurotransmitter release? Cell Calcium 43:9–15.
51. Vyleta NP and SM Smith. (2011). Spontaneous glutamate release is independent of calcium influx and tonically activated by the calcium-sensing receptor. J Neurosci 31:4593–4606.

Address correspondence to:
Dr. Shan Ping Yu
Department of Anesthesiology
Emory University School of Medicine
101 Woodruff Circle
Woodruff Memorial Research Building, Suite 620
Atlanta, GA 30322

E-mail: spyu@emory.edu

Received for publication October 7, 2012
Accepted after revision December 21, 2012
Prepublished on Liebert Instant Online December 23, 2012